

See discussions, stats, and author profiles for this publication at:
<https://www.researchgate.net/publication/13788236>

Effect of Magnesium Ions on the Properties of Foam Films Stabilized with Sodium Dodecyl Sulfate

ARTICLE *in* JOURNAL OF COLLOID AND INTERFACE SCIENCE · DECEMBER 1997

Impact Factor: 3.37 · DOI: 10.1006/jcis.1997.5133 · Source: PubMed

CITATIONS

13

READS

31

5 AUTHORS, INCLUDING:



Jana K Angarska

Konstantin Preslavsky University of Sh...

24 PUBLICATIONS 224 CITATIONS

SEE PROFILE



Krasimir Dimov Tachev

Konstantin Preslavsky University of Sh...

10 PUBLICATIONS 113 CITATIONS

SEE PROFILE

Effect of Magnesium Ions on the Properties of Foam Films Stabilized with Sodium Dodecyl Sulfate

J. K. Angarska,^{*,1} K. D. Tachev,^{*} I. B. Ivanov,[†] A. Mehreteab,[‡] and G. Brose[§]

^{*}University of Shoumen, 9700 Shoumen, Bulgaria; [†]Faculty of Chemistry, University of Sofia, 1126 Sofia, Bulgaria;
[‡]Colgate-Palmolive Technology Center, 909 River Road, Piscataway, New Jersey 09954; and [§]Colgate-Palmolive Research
and Development, Inc., Avenue Du Parc Industriel, B-4041 Milmort (Herstal), Belgium

Received January 7, 1997; accepted August 19, 1997

Unstable and equilibrium foam films and foams formed from solutions of sodium dodecyl sulfate and bivalent electrolyte, MgCl_2 or MgSO_4 , are experimentally investigated. It was found that at low ionic strength and low surfactant concentration the films with magnesium ions are more stable than films with sodium ions. At higher surfactant concentration the films containing MgCl_2 become stable while the films with MgSO_4 remain unstable. The unstable films exhibit at least five types of rupture which are documented by photographs and frequency distribution curves of the film lifetimes. In the case when magnesium ions are present the formation of lenses inside the film was observed; the lenses contribute to a longer lifetime of the films. With the stable films the transition from common to Newton black film occurs at magnesium concentrations between 0.01 and 0.015 M . The results for the stability of single microscopic films are found to correlate with the results for the foam drainage. © 1997 Academic Press

Key Words: thin liquid films; bivalent ions; film lifetime; critical thickness of film rupture; foam; critical electrolyte concentration of transition to Newton black film.

1. INTRODUCTION

The *equilibrium* properties (e.g., film thickness and contact angle) of thin liquid films (TLF) are expected to play a role for the foam stability. In addition, the *nonequilibrium* parameters, the lifetime of the film and the critical thickness of rupture, also play an essential role. The equilibrium properties might be of importance for relatively stable foams, i.e., foams generated from solution of high surfactant concentration. The nonequilibrium properties are important for unstable foams produced at low surfactant concentration. Foam films stabilized with different surfactants have been studied intensively for many years (1–6). Such investigations have been used to check the applicability of the DLVO theory of film stability (1) or to confirm and analyze the theoretical predictions for the film thinning (7–9), rupture (10, 11), structure (1, 2, 5), transition from common black

film (CBF) to Newton black film (NBF) (2, 4), etc. At the present time a reach set of data for the film thickness, contact angle, surface free energy, and other thermodynamic properties of films from sodium dodecyl sulfate (SDS) solutions in the presence of *monovalent* electrolytes has been collected under a wide range of experimental conditions (2, 3). It is believed that these properties of TLF are closely related to the foamability, foam growth, drainage of liquid from a foam, foam stability, etc. (12).

At the same time no systematic investigation of films at low ionic strength created by *bivalent* ions is available. Such ions are present for instance in tap water which is of great practical importance for foaming systems. Magnesium and calcium ions as well as carbonate and phosphate coions present in tap water are responsible for its hardness, which is known to affect strongly the foaminess of surfactants (13). However, the way in which multivalent ions, i.e., water hardness, play a role in the foam stability is far from being clear. Hence, a study of TLF in the presence of bivalent ions at low electrolyte concentrations can be useful for understanding this mechanism.

In the present study we carried out two types of experiments with microscopic foam films formed in a glass capillary (1) and stabilized with SDS. The first type are experiments with unstable films containing magnesium ions at low ionic strength of 0.024 M provided by electrolytes with different coions: MgCl_2 or MgSO_4 . In these experiments the concentration of SDS is varied from 8.75×10^{-5} to 8×10^{-4} M at a fixed concentration of MgCl_2 or MgSO_4 (0.006 M). To have a reference system we performed also experiments with TLF containing NaCl. Several different types of film thinning and rupture have been observed with the films containing magnesium ions. Some of them resemble the evolution of films with monovalent electrolyte, whereas others, e.g., when there is an appearance of lenses inside the film, seem to be a peculiarity of the films with bivalent ions.

As the thinning and the stability of single foam films are important factors for the foam stability, a study of real foams was done in order to compare the film properties with the parameters of the foam drainage and destruction.

¹ To whom correspondence should be addressed. Fax: (54)-63171.
E-mail: angarska@uni-shoumen.bg.

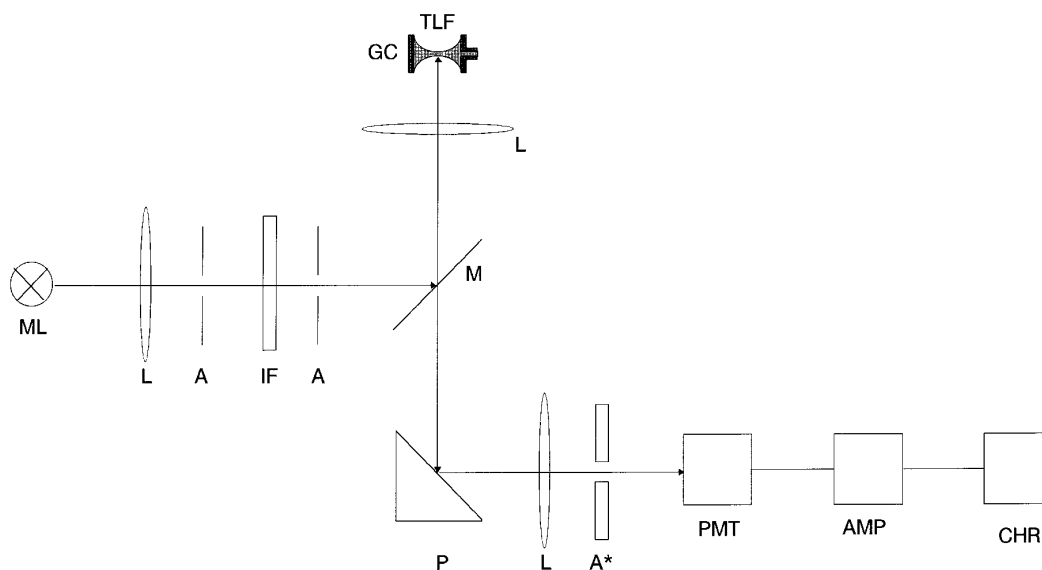


FIG. 1. Experimental setup for investigation of thin liquid films consisting of glass cell (GC) for formation of TLF, optical microscope (mercury lamp, ML; lenses, L; apertures, A; interference filter, IF; semitransparent mirror, M; prism, P), and detecting system (aperture, A*; photomultiplier, PMT; amplifier, AMP; chart recorder, CHR).

The second type of experiment was with stable films. In this case the concentration of Mg^{2+} was varied from 0.006 to 0.043 *M* at a fixed concentration of SDS, 5.8×10^{-3} *M*, in order to determine the critical concentration of transition from CBF to NBF. Such information was not known for Mg^{2+} . This transition occurs in a concentration range from 0.01 to 0.015 *M*. For stable SDS films with bivalent electrolytes we present also data about their equilibrium contact angle and film thickness. The film properties are different when MgCl_2 or MgSO_4 is present in the solution. These data can serve as a basis for theoretical treatment. Since the bivalent ions are known to bind strongly to adsorbed surfactant monolayers (14), they can affect significantly the intermolecular interactions in the film originating from non-DLVO forces affecting the NBF stability (15). More appropriate for theoretical treatment is symmetrical electrolyte (MgSO_4).

The observed differences between the film properties in the presence of symmetrical (MgSO_4) and nonsymmetrical (MgCl_2) electrolyte can be attributed to the effect of the coions.

2. EXPERIMENTAL

a. Experimental Setup

The properties of the thin liquid films were studied by the interference technique developed originally by Scheludko and Exerowa (1). A sketch of the experimental setup used by us is shown in Fig. 1. The foam film is formed in a glass cell by sucking out the liquid from a glass capillary of internal radius 0.189 cm. For this purpose a Teflon microsyringe filled with mercury is used. The cell bottom is made of

plane parallel optical glass. Some amount of the investigated surfactant solution was poured on the cell bottom in order to saturate the air in the cell with water vapor. The distance between the TLF and the surface of the solution at the cell bottom is about 0.5 cm, to provide an equilibrium vapor pressure at the level of the film. The glass cell was mounted on the stage of a metallographic optical microscope (Epitip 2, Carl Zeiss, Jena). The cell is closed in a thermostatic jacket (not depicted in Fig. 1) to maintain constant temperature throughout the experiment. The film was observed from below in reflected light by an objective 6.3 \times . The intensity of the monochromatic light (wavelength $\lambda = 551$ nm) reflected from the film was recorded by a photomultiplier and chart recorder.

b. Experimental Procedures

The thickness of stable films, h_e , and the critical thickness of unstable films, h_{cr} , were determined interferometrically from the intensity of the reflected light (16). When the films were unstable the lifetime, τ , was measured by an electronic timer. In the latter case at least 50 films were formed and studied for each solution. The contact angle, θ , of a CBF was obtained from the interference fringes arising at the film periphery. The positions of the fringes were measured from the photographs taken by replacing the detecting system by a photcamera. The profile of the film periphery was reconstructed from the photographs and the contact angle was calculated by a numerical procedure, based on the Laplace equation of capillarity (17). The contact angle of NBF was determined by the so-called expansion method (7) based on the observation that during the transition from CBF to NBF no additional liquid is sucked out from the film meniscus.

Assuming that the total volume of the meniscus and the film remains constant during this transition one can calculate the contact angle of the NBF from the respective geometrical formulae by iterations (7).

In this study the drainage of liquid from wet foams was investigated. Wet foam was generated by the Bartsch method in a glass cylinder of total volume 150 cm³. Each solution investigated (with a volume of 20 cm³) was shaken 20 times by hand as uniformly as possible. Immediately after that the cylinder was put in vertical position on a horizontal table and the volume of the liquid under the foam (the so-called "initial volume," V_0) or the height of the foam (initial foam height, h_0) was measured. Since the liquid drains out from the foam fast, the times for reaching certain volumes of the drained liquid have been recorded in order to obtain enough data points from the initial stages of foam drainage. At least five independent measurements of these times were carried out for each investigated solution. The data were then averaged. The measuring of the actual foam height as a function of time was not possible because of the irregularities of the foam breakage. That is why we estimated the integral time for the foam destruction, τ_{br} . It is defined as the time elapsed from the moment of the foam formation up to the appearance of a bare liquid surface at the center of the cylindrical container.

The volume of the liquid drained out of the foam as a function of time was fitted by a double exponential equation (18),

$$V(t) = V_\infty - V_1 \exp\left(-\frac{t}{\tau_1}\right) - V_2 \exp\left(-\frac{t}{\tau_2}\right), \quad [1]$$

where $V_\infty = 20$ ml is the drained liquid volume at infinite time, V_1 and V_2 are parameters obeying the condition $V_1 + V_2 = V_\infty - V_0$; τ_1 and τ_2 are characteristic times of the foam drainage. It is assumed that the time constant τ_1 accounts for the gravity driven drainage of the liquid from the foam, whereas τ_2 reflects the coalescence of foam bubbles due either to the diffusion of air across the foam lamellae or to the rupture of thin films between the bubbles. In the presented study V_1 , V_2 , τ_1 , and τ_2 are determined from the data for $V(t)$ as adjustable parameters by a minimization procedure.

The surface tension of the surfactant solutions was measured by the Wilhelmy plate method.

c. Materials

Sodium dodecyl sulfate (p.a. grade, from Sigma) was used as surfactant. Sodium chloride, NaCl (p.a. grade, from Merck), magnesium chloride, $\text{MgCl}_2 \cdot 6\text{H}_2\text{O}$, and magnesium sulfate, $\text{MgSO}_4 \cdot 7\text{H}_2\text{O}$ (both p.a. grade, from Teokom, Bulgaria), were used as electrolytes. The solutions were prepared with double distilled water.

d. Experimental Conditions

Unstable films were formed from solutions of SDS below the critical micelle concentration (CMC) in the range from

8.75×10^{-5} to 8.0×10^{-4} M. The experiments were performed at ionic strength of 0.024 M. The concentration of MgCl_2 or MgSO_4 was constant, equal to 0.006 M. This concentration corresponds to the concentration of bivalent metal ions in the hard water. Since the $\text{MgCl}_2 \cdot 6\text{H}_2\text{O}$ and $\text{MgSO}_4 \cdot 7\text{H}_2\text{O}$ are highly hygroscopic, stock solutions of MgCl_2 and MgSO_4 were prepared. The exact concentrations of Mg^{2+} ions were determined by titration. In the solutions of SDS containing MgCl_2 at the ionic strength of 0.024 M was achieved by adding some amount of NaCl. In order to compare the effects of bivalent and monovalent counterions, experiments with NaCl as electrolyte at the same ionic strength were carried out.

For the sake of comparison, additional experiments at a higher concentration of Mg^{2+} (0.043 M) were performed. This concentration corresponds to ionic strength 0.128 M in solutions containing MgCl_2 and to ionic strength 0.172 M in solutions with MgSO_4 .

In the study of equilibrium films we used solutions with a constant concentration of SDS (5.8×10^{-3} M) which is above CMC. In these cases the concentration of Mg^{2+} was varied from 0.006 to 0.043 M. The concentration of Na^+ ions due to the micelle dissociation (with degree of dissociation of a micelle $\alpha = 0.146$) was taken into account when the ionic strengths of these solutions were calculated.

3. RESULTS

a. Unstable Films

Table 1 presents the measured lifetime and the critical thickness of rupture of the unstable films. The values of the equilibrium surface tension of the solutions are also shown. It was observed that film drainage and rupture can progress in a different way depending on the experimental conditions. Moreover, we witnessed that alternative mechanisms of film rupture exist even for films formed under the same experimental conditions. We distinguish five types of film rupture, depicted schematically in Fig. 2:

(i) Rupture of *bright* film preceded by formation of small gray spot(s). This type predominates at low SDS concentrations despite of the type of the counterion. When the film reaches a thickness ≥ 50 nm one or more small dark grey spot(s) appear near the film periphery and quickly move randomly for about 1–2 s, immediately after which the film breaks down.

(ii) Rupture of *gray* film. The film thins gradually up to thickness ranging from 15 to 36 nm for several tens of seconds and suddenly ruptures (Fig. 3a).

(iii) Rupture of dark gray film containing *lenses*. The lenses appear in a group during the transition from gray to dark gray film of thickness close to 25 nm. The lenses look like bright circular spots several micrometers in diameter. They are dispersed mainly in the central zone of the film and move randomly throughout the film. Their size and their

TABLE 1
Experimental Parameters of Liquid Films Stabilized with SDS in the Presence of Different Electrolytes

| C_{SDS} ($\times 10^4 M$) | Ionic strength | Type of rupture | Lifetime τ (s) | | | Critical thickness of rupture h_{cr} (nm) | | Surface tension σ (mN/m) | | |
|---|-------------------|-----------------------|---------------------|-------------------|-------------------|---|-------------------|---------------------------------|-------------------|-------------------|
| | | | NaCl | MgCl ₂ | MgSO ₄ | MgCl ₂ | MgSO ₄ | NaCl | MgCl ₂ | MgSO ₄ |
| 0.875 | 0.024 | I | 4.8 | 20.1 (63%) | 15.9 (50%) | 16.5 | ≈ 50 | 63.0 | 51.9 | 59.6 |
| | | II | | 41.6 (37%) | | | | | | |
| | | III | | | 89.4 (50%) | | 25.0 | | | |
| | | IV | | | | | | | | |
| | | V | | | | | | | | |
| 2.0 | 0.024 | I | 12.2 | 21.0 (58%) | | 44.1 | | 57.2 | 47.7 | 49.9 |
| | | II | | 41.5 (42%) | 38.4 (75%) | | 36.1 | | | |
| | | III | | | | | | | | |
| | | IV | | | 67.4 (25%) | | 21.9 | | | |
| | | V | | 33.4 | | | | | | |
| 4.3 | 0.024 | I | Stable | | | 45.5 ^a | | 48.9 | 40.1 | 46.4 |
| | | II | | | | | | | | |
| | | III | | | | | | | | |
| | | IV | | | | | | | | |
| | | V | | | | | | | | |
| 8.0 | 0.024 | I | Stable | | | 13.2 | | 31.1 | 32.8 | 41.9 |
| | | II | | | | | | | | |
| | | III | | | | | | | | |
| | | IV | | | | | | | | |
| | | V | | | | | | | | |
| 8.0 | 0.128 | I | Stable | | | 50.2 | | 44.8 | 34.9 | 38.8 |
| | | II | | | | | | | | |
| | | III | | | | | | | | |
| | | IV | | | | | | | | |
| | | V | | | | | | | | |
| 8.0 | 0.172 | I | Stable | | | 269.3 | | 32.0 | 32.0 | 35.6 |
| | | II | | | | | | | | |
| | | III | | | | | | | | |
| | | IV | | | | | | | | |
| | | V | | | | | | | | |
| 8.0 | 0.172 | I | Stable | | | 56.6 | | 32.0 | 32.0 | 35.6 |
| | | II | | | | | | | | |
| | | III | | | | | | | | |
| | | IV | | | | | | | | |
| | | V | | | | | | | | |

^a Film thickness just in the moment of Newton black spot appearance.

number decrease with time due to coalescence. The film ruptures when only a few lenses are still present in the film. This type of rupture was observed only at a SDS concentration of $8.75 \times 10^{-5} M$ in the presence of MgSO_4 .

(iv) Rupture of CBF during the transition to NBF. This type was found at higher surfactant concentrations in the presence of magnesium ions. In this case the lenses appear during the transition to a film of thickness about 18 nm (Fig. 3b). The lenses are more pronounced than in type (iii) and live longer (up to 3–4 min). In some cases their evolution ends with the formation of a single lens which either vanishes gradually or merges the film meniscus. Once the lenses disappear the transition to NBF begins. The film ruptures soon after never reaching a state of stable NBF. In other cases the rupture occurs during the transition to NBF when several lenses are still present inside the film.

(v) Rupture of NBF. This type of behavior was observed only at $0.043 M \text{Mg}^{2+}$. The transition to NBF starts before the transition from gray film to CBF is completed (Fig. 3c). The lifetime of NBF is only few seconds.

The lifetimes of films formed from each solution (at least 50 films) were split into groups according to the observed types of film rupture which depend on the surfactant concentration and on the concentration and the type of electrolyte. After that we determined the time interval, $\tau_{\text{max}}^k - \tau_{\text{min}}^k$, and split it into equal time intervals $\Delta\tau$ whose duration was taken close to $\sqrt{N^k}$. Here τ_{max}^k and τ_{min}^k are the maximum and the minimum lifetime, respectively, and N^k is the number of films exhibiting k th type of rupture ($k = \text{i, ii, iii, iv, v}$). The frequency distribution curves were then obtained as the percentages of the number of films N_{τ}^k (with lifetimes

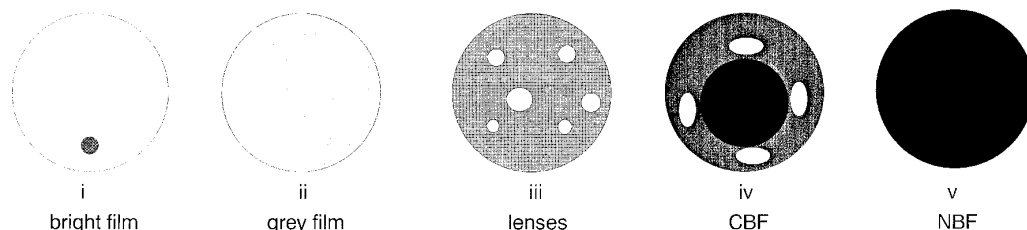


FIG. 2. Different types of rupture of microscopic foam films depicted as the final states just before the film breaks.

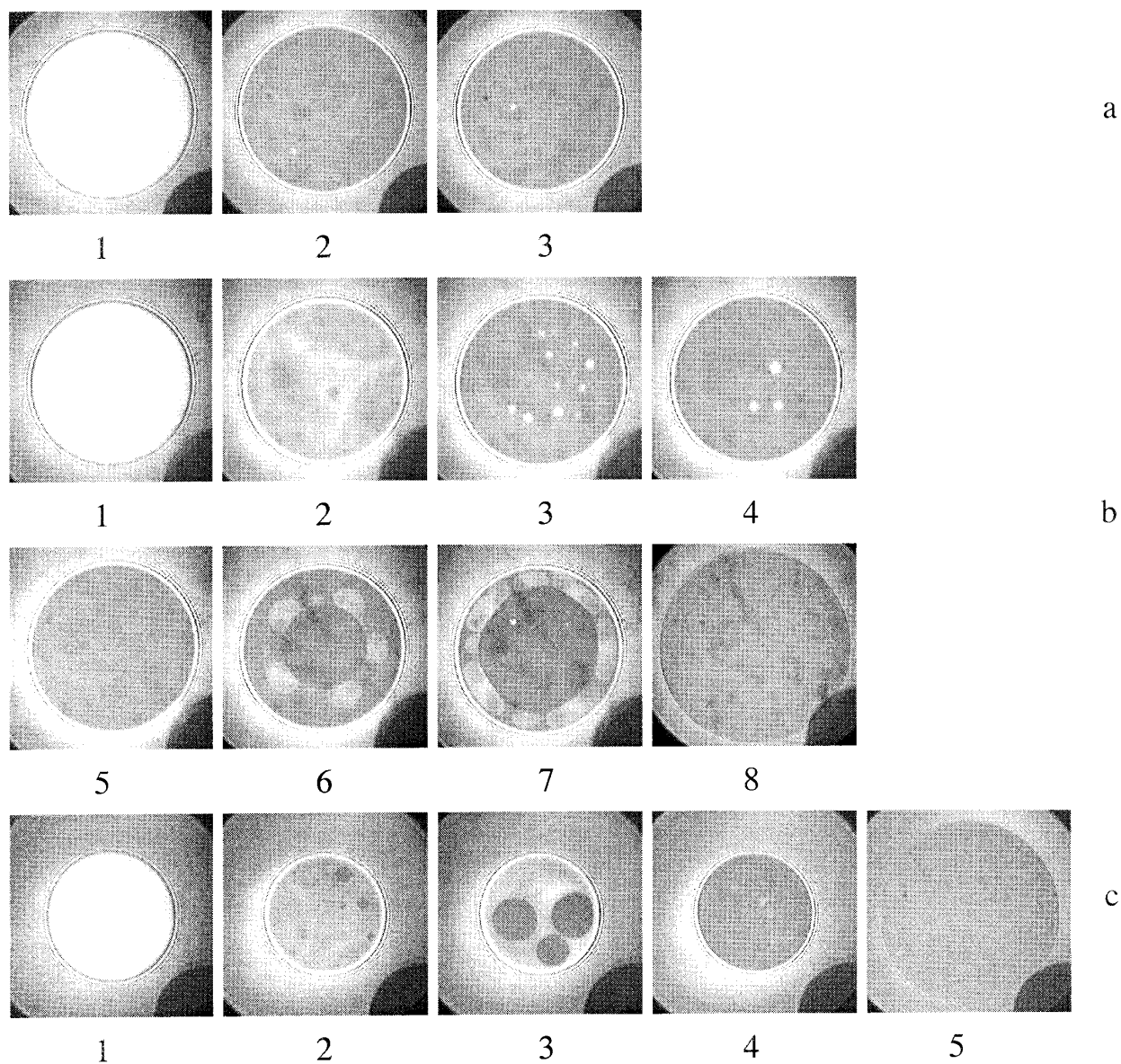


FIG. 3. Photographs of the successive stages of films following different type of rupture: (a) type (iii), $8.75 \times 10^{-5} M$ SDS, $0.006 M$ $MgSO_4$; (b) type (iv), $8.0 \times 10^{-4} M$ SDS, $0.006 M$ $MgSO_4$; (c) type (v), $8.0 \times 10^{-4} M$ SDS, $0.043 M$ $MgSO_4$.

falling into a particular interval $\Delta\tau$) were plotted as functions of time. In Table 1 the characteristic lifetimes of the films, τ , are shown (the so-called medians of the distribution curves), where the time τ separates the area below the distribution curve into two equal parts, i.e., $\sum N_{\tau}^k = N_k/2$. In our experiments this time is more representative than the mean lifetime, $\sum \tau^k/N_k$, which tends to an overestimation of the long-living film contribution. In parentheses the percentages of films following the k th type of rupture are presented. The frequency distribution curves of the observed types of rupture are plotted in Fig. 4. One can see that while the curves for types (i), (ii), and (v) are symmetric and with a shape close to the normal distribution, the curves for types (iii) and (iv) are asymmetrical with bigger dispersion due to the longer living films with lenses.

b. Stable Films

In Fig. 5 the experimental data for h_e and θ are plotted vs the concentration of $MgSO_4$. Transition from CBF to NBF is seen at concentrations of bivalent electrolyte exceeding $0.01 M$ where the contact angle and the film thickness change dramatically. Since up to a concentration of $0.015 M$ this transition was not always observed there is a transition region rather than a critical concentration of transition. The rate of expansion of the initial Newton black spot with $MgSO_4$ is much lower than the corresponding rate in films with $MgCl_2$ where the transition was almost instantaneous. That is why it was impossible to determine the contact angles of CBF for $MgCl_2$. The respective contact angles of NBF were calculated by the expansion method

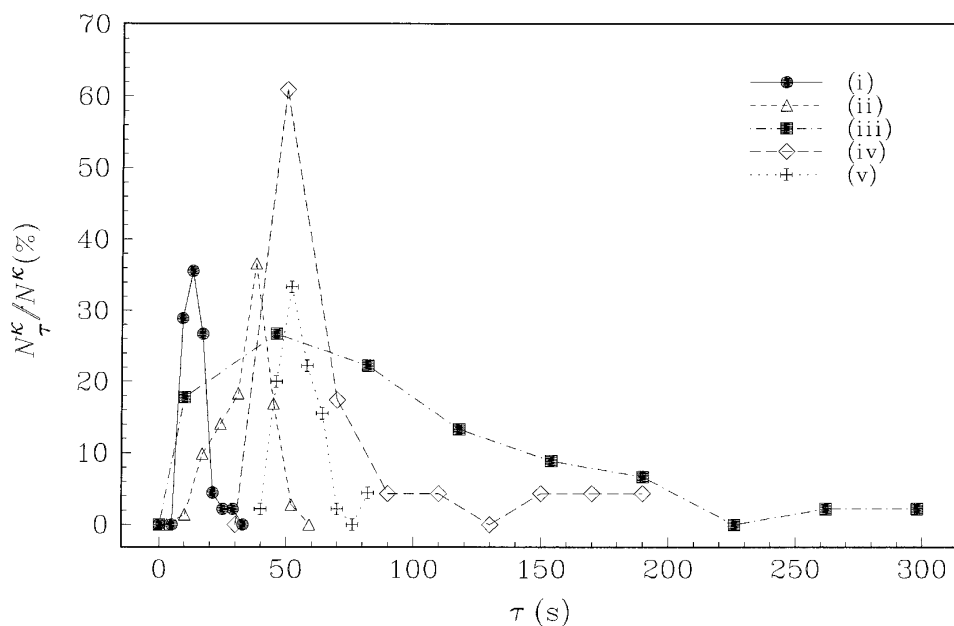


FIG. 4. Frequency distributions of the lifetimes, τ , of films obeying different types of rupture in the presence of magnesium ions: type (i), SDS concentration $8.75 \times 10^{-5} M$; type (ii), $2 \times 10^{-4} M$ SDS; type (iii), $8.75 \times 10^{-5} M$ SDS; type (iv), $8 \times 10^{-4} M$ SDS, $0.006 M$ $MgSO_4$; type (v), $8 \times 10^{-4} M$ SDS, $0.043 M$ $MgSO_4$.

(7), assuming that the contact angle of CBF is equal to zero at the moment of transition. The obtained values were close but higher than the ones depicted in Fig. 5 for NBF with $MgSO_4$. Similarly, the equilibrium thicknesses of NBFs with $MgCl_2$ were close but smaller than the respective thicknesses of films with $MgSO_4$.

c. Foams

It is known that the thinning and the stability of single liquid films are important factors for foam stability. For this

reason the study of the foam films was complemented by experiments with real foams. This would give the opportunity to check the correlation between the drainage and stability of foams produced from SDS solutions with monovalent and bivalent electrolytes and the behavior of microscopic films formed from the same solutions.

The volume of the liquid draining out of the foam is plotted as a function of time on Figs. 6 and 7.

Figure 6 presents the results for foams produced from

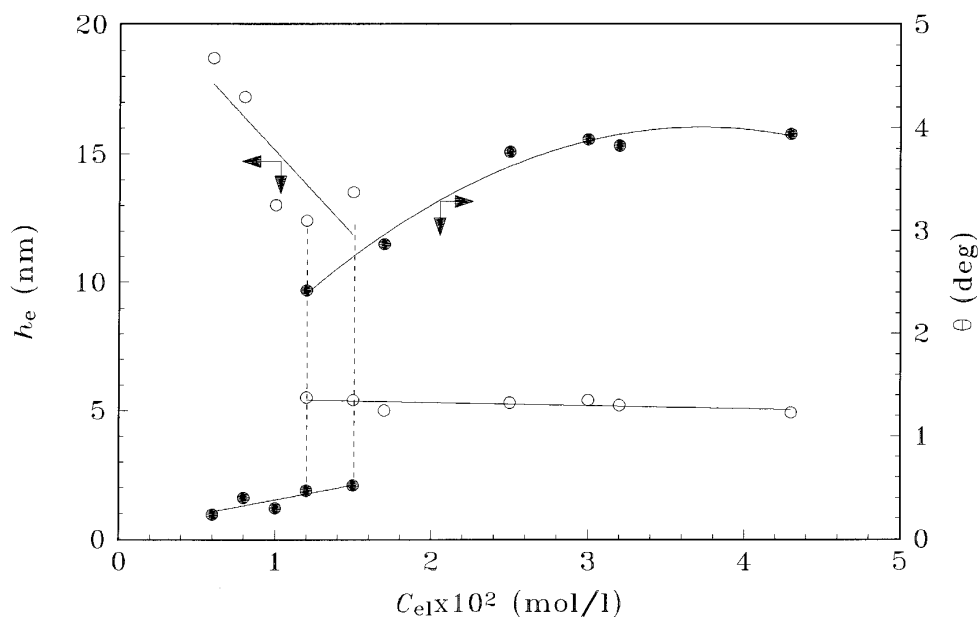


FIG. 5. Equilibrium film thickness, h_e (open circles), and contact angle, θ , (solid circles) vs electrolyte ($MgSO_4$) concentration, C_{el} , at $5.8 \times 10^{-3} M$ SDS. The region of transition from CBF (left) to NBF (right) is located between the two dashed lines. The solid lines are drawn to guide the eyes.

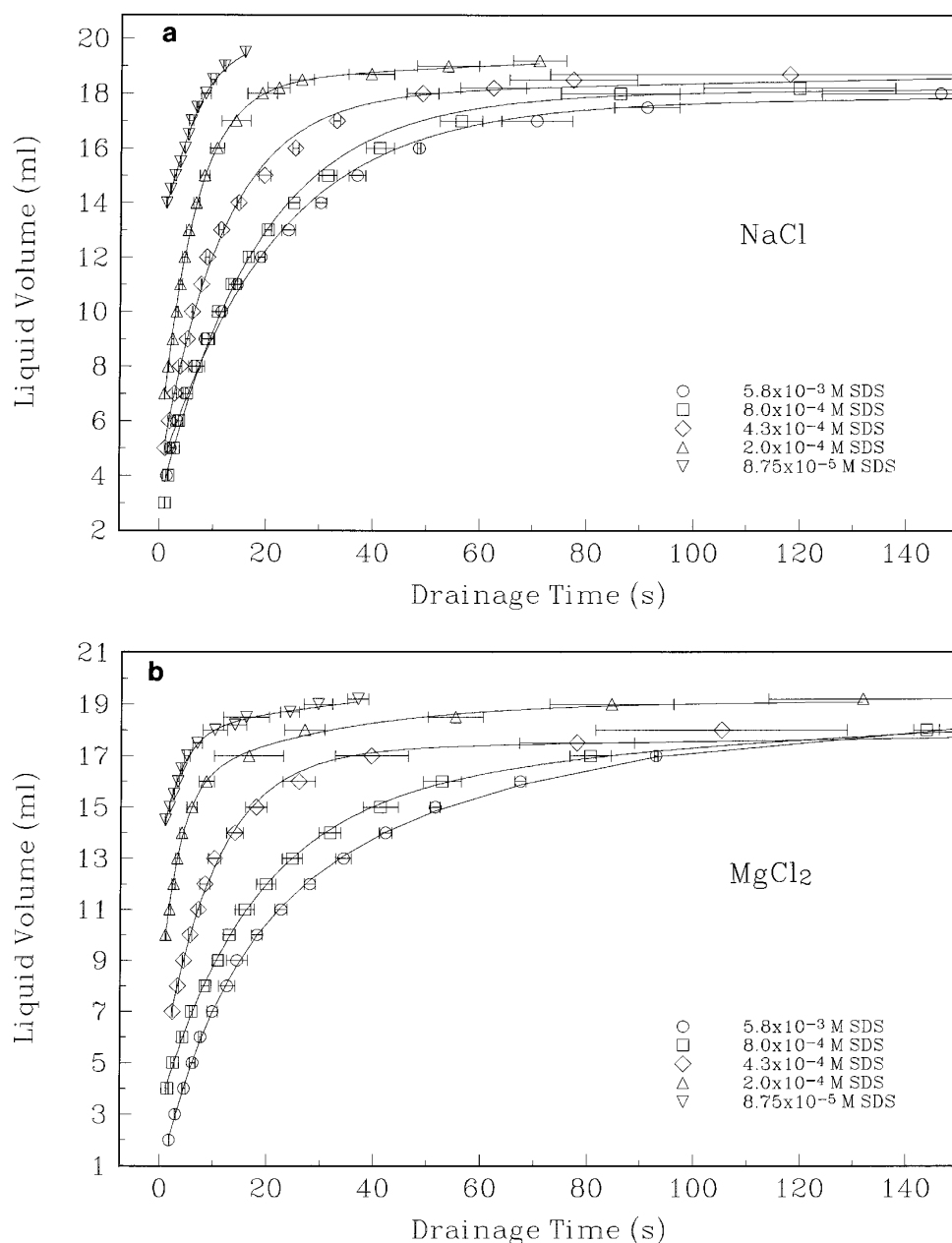


FIG. 6. Drainage of the liquid from foam produced from solutions of different SDS concentrations with: (a) NaCl, (b) MgCl₂, (c) MgSO₄. The ionic strength of all solutions was 0.024 M.

solutions with different SDS concentrations in the presence of NaCl (Fig. 6a), MgCl₂ (Fig. 6b), and MgSO₄ (Fig. 6c) at a constant ionic strength of 0.024 M.

In Fig. 7 the results for foams generated from solutions at 2×10^{-4} M SDS and ionic strength 0.024 M maintained by different electrolytes are shown.

Table 2 presents the results for the initial liquid volume (V_0), initial foam height (h_0), and the integral time (τ_{br}) of the foam breakage obtained experimentally.

The foams produced from all of the solutions studied were unstable except the foams from 5.8×10^{-3} M SDS irrespectively of the electrolyte type. The initial rate of

the foam drainage decreases with the increase of the concentration of SDS but the valence of the counterion does not affect it. The most unstable were the foams with NaCl (with the smallest τ_{br}) although the foamability of these solutions were the highest according to the values of V_0 and h_0 (Table 2). It was found that the replacing of Na⁺ with Mg²⁺ leads to a decrease of the foamability of solution (higher V_0 and lower h_0) and to an increase of the foam lifetime (higher τ_{br}). The foams from 5.8×10^{-3} M SDS were stable in the presence of all electrolytes used. They drained fast and after half an hour remained completely dry with a constant height.

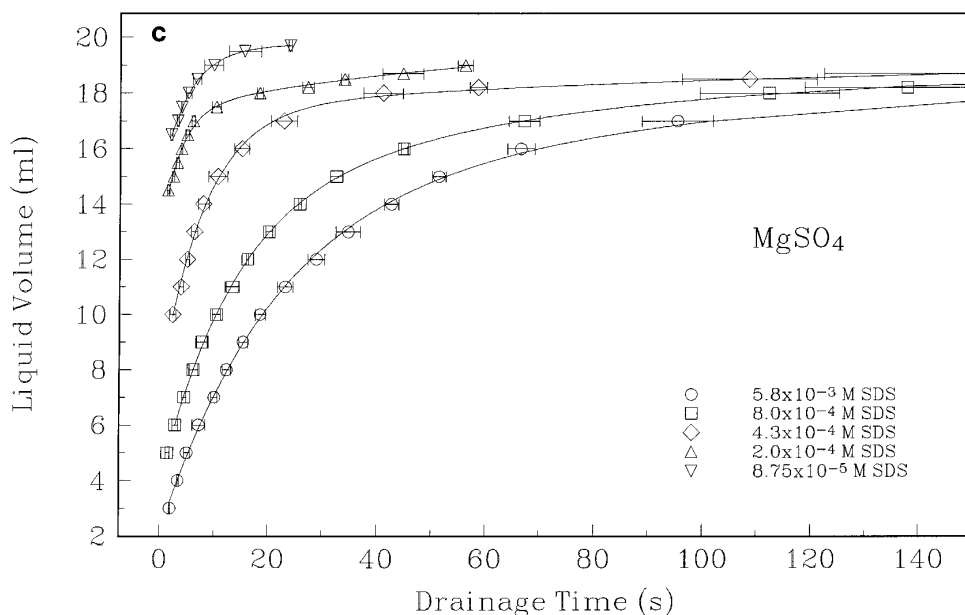


FIG. 6—Continued

4. DISCUSSION

a. Unstable Films

One can see from Table 1 and Figs. 2 and 3, the unstable foam films containing *bivalent* ions exhibit stages of thinning and rupture, which are similar to what is known from the experiments with films from solutions containing 1:1 electrolyte. For example, one observes relatively thick films with uneven thickness, films reaching a state of instability by

forming common black or Newton black spots (1), and rupturing of unstable NBF (11, 19). Comparing the lifetime of predominant types of film rupture, horizontally and vertically in Table 1, one can outline the following trends:

- At low SDS concentrations ($8.75 \times 10^{-5} M$, $2.0 \times 10^{-4} M$), the film lifetime increases three to four times and the critical thickness of film rupture diminishes when the monovalent electrolyte (NaCl) is replaced with bivalent one ($MgCl_2$ or $MgSO_4$). This tendency is clearly demonstrated

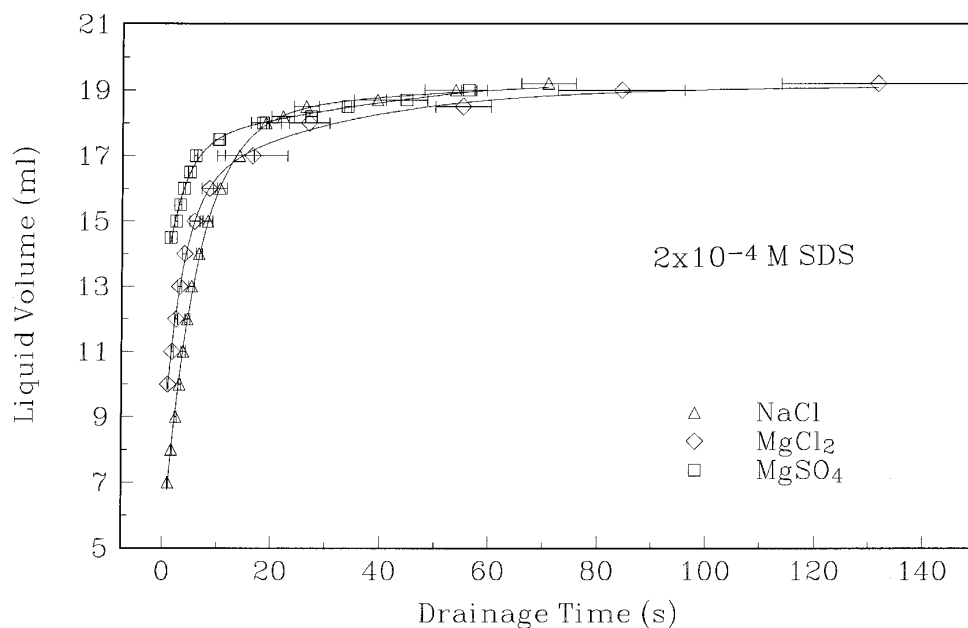


FIG. 7. Drainage of the liquid from foam produced from solutions with $2 \times 10^{-4} M$ SDS in the presence of different electrolytes with ionic strength 0.024 M.

TABLE 2
Initial Foam Volume (V_0), Initial Foam Height (h_0), and Integral Time (τ_{br}) for Foam Breakage of SDS Foams in the Presence of Different Electrolytes at Constant Ionic Strength of 0.024 M

| C_{SDS} ($\times 10^{-4} M$) | V_0 (ml) | | | h_0 (ml) | | | τ_{br} (s) | | |
|-------------------------------------|------------|-------------------|-------------------|------------|-------------------|-------------------|-----------------|-------------------|-------------------|
| | NaCl | MgCl ₂ | MgSO ₄ | NaCl | MgCl ₂ | MgSO ₄ | NaCl | MgCl ₂ | MgSO ₄ |
| 0.875 | 13.0 | 14.0 | 16.0 | 33.8 | 31.0 | 29.8 | 15.2 | 33.0 | 24.0 |
| 2.0 | 6.0 | 9.0 | 14.0 | 45.0 | 40.0 | 39.8 | 77.7 | 131.6 | 56.4 |
| 4.3 | 4.0 | 4.0 | 6.3 | 65.0 | 54.3 | 45.0 | 627 | 1641.0 | 795.0 |
| 8.0 | 2.0 | 3.0 | 3.0 | 88.0 | 80.0 | 71.8 | 1630 | >7200 | >7200 |

Note. The concentration of magnesium ions was 0.006 M .

in Fig. 8 by the distribution curves of type (i), predominating for films with $8.75 \times 10^{-5} M$ SDS. A possible explanation is that the Mg^{2+} ions interconnect the negatively charged headgroups of SDS at the film surfaces, thus increasing the surface elasticity and viscosity; the latter effects tend to “solidify” the film surfaces and to oppose the drainage of the liquid out of the films. The existence of lenses in the film in this case provides a reservoir of liquid and increases the film drainage time (see below for details).

• In contrast, at a higher surfactant concentration ($4.3 \times 10^{-4} M$) Mg^{2+} ions have a destabilizing effect. For instance, the films are stable in the presence of Na^+ , whereas the exchange of Na^+ with Mg^{2+} leads to unstable CBFs which rupture during the transition to NBFs. Indeed, for the higher SDS concentration the film surfaces are immobilized by the dense adsorption monolayers; hence the effect of the Mg^{2+} ions on the surface rheology (see the previous case) cannot show up. On the other hand, the bivalent Mg^{2+} ions should

be expected to adsorb stronger in the subsurface Stern layer, thus partially neutralizing the surface charge and suppressing the electrostatic repulsion. Moreover, the Mg^{2+} ions give rise to an additional ionic correlation attraction between the film surfaces (27, 28).

• At $8.0 \times 10^{-4} M$ SDS the films with $MgCl_2$ become stable while films with $MgSO_4$ remain unstable which is an intriguing effect of the coions on the film thinning and stability.

• At higher electrolyte concentrations (0.128 M NaCl and 0.043 M Mg^{2+}) only films with $MgSO_4$ are unstable which points out again the role of the coions.

• The predominating type of film rupture is determined by the type and concentration of the electrolyte as well as by the concentration of SDS.

The above trends can be explained, at least qualitatively, by the theories for rupture of TLF. The theory of the ther-

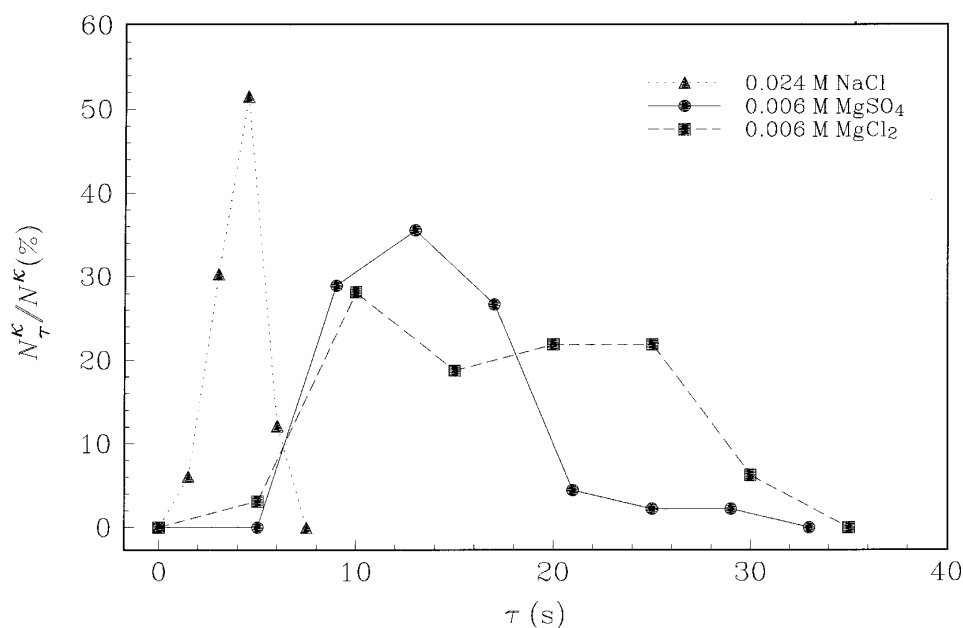


FIG. 8. Frequency distribution curves for the films obeying the type (i) of rupture in the presence of different electrolytes with ionic strength of 0.024 M .

mally excited capillary waves attributes the film rupture to waves appearing along the film surfaces (9, 10, 20–24). If two waves of certain amplitudes simultaneously appear against each other on the two film surfaces, they can lead to instability, resulting in a local contact of the two film surfaces and rupture of the film. This local contact is facilitated by negative (attractive) disjoining pressure leading to additional attraction between the film surfaces. By counterbalancing the different forces acting in the film one can determine the critical thickness of film rupture, h_{cr} , which can be measured experimentally. If the rate of film thinning is also known, one can calculate the lifetime of the film. However, some films can live at constant thickness longer than expected due to damping of the capillary waves (dense adsorption layers) or repulsion between film surfaces (positive disjoining pressure).

For the very thin NBFs another mechanism of film rupture was proposed (11, 19). It assumes formation of vacancies in the surfactant adsorption monolayers. Coalescing vacancies increase in size until a hole of critical size forms which provokes destruction of the film.

Below we will compare our experimental results with the predictions of the theories of film rupture and present in more detail some of the possible explanations mentioned above.

At low surfactant concentration the films are generally unstable (type (i)), especially in the presence of sodium ions. Due to the lower density of the adsorption monolayers the capillary waves existing on the film surfaces can readily reach the amplitude required to destroy the film. With the increase of the surfactant concentration the adsorption monolayers become saturated, which leads to damping of the capillary waves (8, 24). The decreased amplitude of the waves allows the films to reach lower critical thickness of rupture. At the same time, the value of the surface potential increases due to increased surface charge which provokes additional repulsive (stabilizing) disjoining pressure (8, 9). Probably this is the reason thinning of the films to cease with CBF-state at 4.3×10^{-4} M SDS.

The adsorption layers can also be tightened to damp effectively the capillary waves by replacing sodium ions with magnesium ions. The stabilizing role of Mg^{2+} at lower concentrations of SDS (Table 1) is probably because of competitive binding of Mg^{2+} to dissociated surfactant headgroups in the adsorption layer due to their larger electric charge (Fig. 9). If Mg^{2+} enters the Stern layer it neutralizes the charge of two DS^- ions, thus decreasing the electrostatic repulsion between their polar heads. This facilitates additional adsorption of SDS molecules, increasing the density of the adsorption layer and its elasticity (25), which can lower the rate of thinning of the film (9). The adsorption of Mg^{2+} also decreases the surface potential and, because of the lowered electrostatics, the films thin to a stage of NBF and then break down due to insufficient repulsion.

As shown above, the films with $MgCl_2$ and $MgSO_4$ exhibit

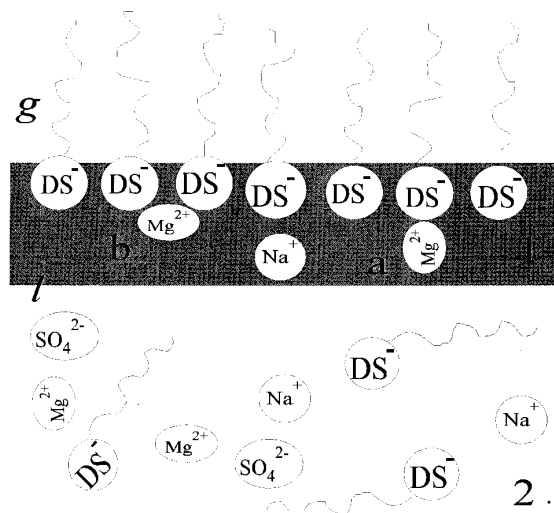


FIG. 9. Scheme of a possible mechanism of adsorption of Mg^{2+} on the interface.

different behavior at 8×10^{-4} M SDS. In the presence of $MgCl_2$, the films were stable and reached a state of NBF with a final thickness of 6 nm while the films with $MgSO_4$ ruptured at the moment of appearance of Newton black spot. Part of these films live 1–2 min after reaching the NBF state. The breakage of films with $MgSO_4$ at this surfactant concentration and stable adsorption layers can be attributed to the formation of local inhomogeneities (Newton black spot) (9) or to the nucleation model with the hole formation (11, 19).

In order to relate the difference between the stability of films with $MgCl_2$ and $MgSO_4$ to the properties of their adsorption layers, we investigated the surface tension of SDS in the presence of magnesium salts (25). According to that data at 8×10^{-4} M SDS the solutions with $MgCl_2$ turned out to be very close to the CMC (9.0×10^{-4} M SDS). The concentration of 8×10^{-4} M SDS is almost two times smaller than CMC (1.3×10^{-3} M SDS) in the presence of $MgSO_4$. The surface tension with $MgCl_2$, $\sigma = 34.9$ mN/m, is closer to the value of σ for its saturated adsorption layer (32.78 mN/m) than the surface tension in the presence of $MgSO_4$, $\sigma = 38.8$ mN/m. The value of σ for saturated layer with $MgSO_4$ is 33.3 mN/m. The presented data show that the lesser stability of the films with $MgSO_4$ is probably due to the smaller extent of saturation of the film interfaces.

The existence of lenses in the films complicate the mechanism of film rupture. Lenses are observed in films of SDS concentration 4.3×10^{-4} and 8.0×10^{-4} M in the presence of either $MgSO_4$ or $MgCl_2$, although in films with $MgSO_4$ their appearance is more pronounced. At the lower surfactant concentration lenses are observed only in the films with $MgSO_4$. The lenses appear in the film during the transition from relatively thick film of uneven thickness of about 50 nm to black film of thickness ca. 20 nm. At that moment extra water from local nonuniformities in the film, seen as

channels, becomes captured in lenses instead of going out from the film. Once such an ensemble of lenses is formed, their size and number continue to change due to the exchange of liquid among the lenses and with the Plateau border. The mediator of this exchange is the flow through the interior of the liquid film. Hence, one can expect two forces to affect the transfer of liquid. One of them is the capillary pressure which tends to flatten this surface, i.e., to squeeze the liquid out from the lens. The capillary pressure is counterbalanced by the drag force due to the viscous flow of liquid in the film. At constant film thickness the viscous force is reversibly proportional to the channel length, i.e., the distance between the lens and the Plateau border at the film periphery. That is why it is more convenient for the liquid to flow initially from one lens to another one instead of going to the Plateau border. The liquid flows from the smaller lenses to the bigger ones driven by the difference in the capillary pressures. Thus the number of the lenses decreases while their average size increases. This process results in the formation of a big single lens which finally disappears. The kinetics of lens formation will be considered in more detail elsewhere (26).

The lenses prolong substantially the film lifetime by increasing mainly the time of existence of film with constant thickness. This fact reflects the asymmetric shape of the distribution curves of types (iii) and (iv) in Fig. 4. The long-time type of film rupture, coexisting with the short-time type of rupture in films at the same experimental conditions (SDS and MgSO_4 concentration, see Table 1) can be also explained by the lens formation.

Increasing the bivalent ion concentration up to 0.043 M suppresses the formation of lenses which influences sufficiently the film lifetime. The films with MgCl_2 become stable, whereas the films with MgSO_4 switch to type (v) of rupture with smaller lifetime.

b. Stable Films

We observed experimentally that the state of a stable film is reached at different concentrations of SDS depending on the type of added electrolyte (Table 1). Foam films in the presence of MgSO_4 become stable at the highest (more than $1.0 \times 10^{-3}\text{ M}$) surfactant concentrations. The increase of SDS concentration in the investigated solutions does not influence substantially the final (equilibrium) film thickness, h_e . The films with NaCl are thicker ($h_e \approx 19\text{ nm}$), while in the presence of MgCl_2 and MgSO_4 their thickness is 13 and 18 nm, respectively, due to lower electrostatic repulsion and ionic correlation attraction caused by Mg^{2+} . The increase of ionic strength leads to a sharp decrease of the equilibrium thickness and enlargement of the contact angle. The transition region from CBF to NBF ($0.01 - 0.015\text{ M}$) observed for films with $5.8 \times 10^{-3}\text{ M}$ SDS and Mg-salts is at a much smaller electrolyte concentration than the respective (1) critical concentration of transition to NBF for NaCl (0.34 M). In order to illustrate the effect of the magnesium ions on

the transition to NBF we studied films at constant concentration ($5.8 \times 10^{-3}\text{ M}$) of SDS and at constant ionic strength (0.128 M) with three different electrolyte systems. CBF with thickness 11.5 nm and contact angle of 0.61° were obtained from the first solution, containing only NaCl. From the second one, containing 0.006 M MgCl_2 and additional NaCl needed to reach the the same ionic strength, the films were again CBF with thickness 11.2 nm. The third solution was with MgCl_2 only (0.043 M). In this case the equilibrium thickness of the films changed dramatically to 5 nm and a transition to NBF occurred. This implies that the magnitude of h_e is mostly related to the bivalent ion concentration rather than to the total ionic strength.

The values of the equilibrium thickness and the contact angle of NBF with MgCl_2 and MgSO_4 were different. In general, the films with MgCl_2 were thinner and with bigger contact angle. For example, films with 0.015 M MgCl_2 have equilibrium thickness $h_e = 4.7\text{ nm}$ and contact angle $\theta = 3.5^\circ$. The respective values of the films with MgSO_4 were $h_e = 5.4\text{ nm}$ and $\theta = 1.99^\circ$.

The simultaneous quantitative interpretation of h_e and θ of stable NBF cannot be achieved in the framework of classical DLVO theory. That is why a theoretical model accounting for some non-DLVO surface forces inside the film should be employed to explain the data (15). For example, the correlations between ions can lead to an additional attraction between the film surfaces (27, 28). Concerning the Newton black films one should account also for the hydration repulsion (see, e.g., Ref. 29). Moreover, additional short-range repulsion stems from the protrusion of surfactant molecules out of the adsorption monolayers at the film surfaces (30).

c. Foams

In general, the results obtained for the stability of single microscopic films correlate with the results for the foam drainage.

At low SDS concentrations the foams are highly unstable. Their integral times of drainage, τ_{br} (15–130 s), correlate with the predominant types of rupture of films at these concentrations (types (i) and (ii)). As already discussed, some part of the films with MgSO_4 form lenses. However, the decay time of these foams is not prolonged. Probably in the real foam the destruction occurs before lens formation in the foam films, or the lenses merge the Plateau borders faster, forced by their weight insofar as the films in the foam are in general not horizontal.

At higher concentrations of SDS the most unstable turn out to be the foams with NaCl although the microscopic films were stable; this is one more indication for the importance of the factors (surface elasticity and viscosity) stabilizing the films under dynamic conditions. Under the same conditions foams with MgSO_4 live shorter times than foams with MgCl_2 , which correlates well with the observations of single films.

The obtained results can be connected with the measured values of the surface tension (Table 1) which give information for the properties of the adsorption layers. The highest value of σ was obtained for the solutions with NaCl and the lowest one was with MgCl_2 . This allows one to suppose that the tightening of the adsorption layers is different depending on the type of electrolyte. As known, the state of the adsorption layer is of great importance for the hydrodynamic stability which is responsible for the foam lifetime. The large lifetimes of the foams containing Mg^{2+} show the effect of the counterion. While the prolonged destruction of the foams in the presence of MgCl_2 is expected as the films at these conditions are stable, in the presence of MgSO_4 it can be due to the effect of lenses on the thinning and rupture of film inside the foam.

CONCLUDING REMARKS

In this study we present experiments with unstable and stable microscopic films and foams formed from solutions of sodium dodecyl sulfate in the presence of magnesium ions. For the unstable films we measured the lifetime and critical thickness of film rupture at low ionic strength (0.024 M) maintained by monovalent (Na^+) and bivalent (Mg^{2+}) ions varying the SDS concentrations from 8.75×10^{-5} to $8.0 \times 10^{-4}\text{ M}$. We observed different evolution of the films and classified five types of film rupture based on the most typical features of films with Mg^{2+} .

At low SDS concentrations ($8.75 \times 10^{-5}\text{ M}$, $2.0 \times 10^{-4}\text{ M}$), the film lifetime increases three to four times and the critical thickness of film rupture diminishes when the monovalent electrolyte (NaCl) is replaced with a bivalent one (MgCl_2 or MgSO_4) (see Fig. 8). A possible explanation is that the Mg^{2+} ions interconnect the negatively charged headgroups of SDS at the film surfaces, thus increasing the surface elasticity and viscosity. The latter effects tend to immobilize the film surfaces and to oppose the drainage of the liquid out of the films. The existence of lenses in the film in this case provides a reservoir of liquid and increases the film drainage time.

In contrast, at higher surfactant concentration ($4.3 \times 10^{-4}\text{ M}$) the Mg^{2+} ion has a destabilizing effect. For instance, the films are stable in the presence of Na^+ , whereas the exchange of Na^+ with Mg^{2+} leads to unstable CBFs which rupture during the transition to NBFs. Indeed, for the higher SDS concentration the film surfaces are immobilized by the dense adsorption monolayers; hence the effect of the Mg^{2+} ions on the surface rheology (see the previous case) cannot show up. On the other hand, the bivalent Mg^{2+} ions should be expected to adsorb stronger in the subsurface Stern layer, thus partially neutralizing the surface charge and suppressing the electrostatic repulsion. Moreover, the Mg^{2+} ions give rise to an additional ionic correlation attraction between the film surfaces (27, 28).

At $8.0 \times 10^{-4}\text{ M}$ SDS the films with MgCl_2 become

stable while films with MgSO_4 remain unstable, which is an intriguing effect of the coions on the film thinning and stability. At higher electrolyte concentrations (0.128 M NaCl and 0.043 M Mg^{2+}) only films with MgSO_4 are unstable. We hope a future development of the theory of the ionic correlations can give an explanation of the effect of the coions.

We observed experimentally that the state of *stable* film is reached at different concentrations of SDS depending on the type of added electrolyte (Table 1). Foam films in the presence of MgSO_4 become stable at the highest (more than $1.0 \times 10^{-3}\text{ M}$) surfactant concentrations. The increase of SDS concentration in the investigated solutions does not influence substantially the final (equilibrium) film thickness, h_e . The films with NaCl are thicker ($h_e \approx 19\text{ nm}$), while in the presence of MgCl_2 and MgSO_4 their thickness is 13 and 18 nm, respectively, due to lower electrostatic repulsion and ionic correlation attraction caused by Mg^{2+} . The increase of ionic strength leads to a sharp decrease of the equilibrium thickness and enlargement of the contact angle. The values of the equilibrium thickness and the contact angle of NBF with MgCl_2 and MgSO_4 were different. In general, the films with MgCl_2 were thinner and with bigger contact angles.

The results for the stability of single microscopic films are found to correlate with the results for the foam drainage. At low SDS concentrations the foams are highly unstable. Their integral times of drainage, τ_{br} (15–130 s), correlate with the predominant types of rupture of films at these concentrations (types (i) and (ii)). At higher concentrations of SDS the most unstable turn out to be the foams with NaCl although the microscopic films were stable; this is one more indication for the importance of the factors (surface elasticity and viscosity) stabilizing the films under dynamic conditions. Under the same conditions foams with MgSO_4 live shorter times than foams with MgCl_2 , which correlates well with the observations of single films.

ACKNOWLEDGMENTS

This work was supported by Colgate-Palmolive. The authors are indebted to Dr. C. D. Dushkin and to Dr. P. A. Kralchevsky for the stimulating discussions.

REFERENCES

- Scheludko, A., *Ann. Univ. Sofia. Fac. Chim.* **62**, 47 (1968/67).
- de Feijter, J., "Contact Angles in Soap Films." Ph.D. thesis, van't Hoff Laboratory, The Netherlands, 1973.
- Kruglyakov, P. M., in "Thin Liquid Films" (I. B. Ivanov, Ed.), Dekker, New York, 1988.
- Exerowa, D., Kolarov, T., and Khristov, Khr., *Colloids Surf.* **22**, 171 (1987).
- Jones, M. N., Mysels, K. J., and Scholten, P. S., *Trans. Faraday Soc.* **62**, 1936 (1966).
- Huisman, F., and Mysels, K. J., *J. Phys. Chem.* **75**, 489 (1969).
- Scheludko, A., Radoev, B., and Kolarov, T., *Ann. Univ. Sofia. Fac. Chim.* **61**, 137 (1966/67). [in Bulgarian]
- Manev, E., Scheludko, A., and Exerowa, D., *Colloid Polym. Sci.* **252**, 586 (1974).

9. Ivanov, I. B., Radoev, B., Manev, E., and Scheludko, A., *Ann. Univ. Sofia. Fac. Chim.* **64**, 363 (1969/70). [in Bulgarian]
10. Radoev, B., Scheludko, A., Manev, E., *Ann. Univ. Sofia. Fac. Chim.* **75**, 227 (1981). [in Bulgarian].
11. Kashchiev, D., and Exerova, D., *J. Colloid Interface Sci.* **77**, 501 (1980).
12. Kruglyakov, P. M., and Exerova, D., "Foam and Foam Films." Chimia, Moscow, 1990. [in Russian]
13. Harris, J. C., in "Nonionic Surfactants" (M. J. Schick, Ed.), p. 683. Dekker, New York, 1967.
14. Israelachvili, J., "Intermolecular and Surface Forces," p. 237. Academic Press, London, 1992.
15. Paunov, V., Kralchevsky, P., Angarska, J., and Tachev, K., to be published.
16. Kolarov, T., Iliev, L., *Ann. Univ. Sofia, Fac. Chim.* **69**, 107 (1974/75). [in Bulgarian]
17. Dimitrov, A. S., Kralchevsky, P. A., Nikolov, A. D., Wasan, D. T., *Colloids Surf.* **47**, 299 (1990).
18. Kann, K. B., "Capillary Hydrodynamics of Foams." Nauka, Novosibirsk, 1989. [in Russian]
19. Miller, H. J., Balinov, B. B., and Exerova, D. R., *Colloids Surf.* **36**, 339 (1989).
20. Ivanov, I. B., Dimitrov, D., *Ann. Univ. Sofia. Fac. Chim.* **66**, (1971/72). [in Bulgarian]
21. Scheludko, A., *Proc. K. Ned. Akad. Wet. B* **65**, 76 (1962).
22. Vrij, A., *Discuss. Faraday Soc.* **42**, 23 (1966).
23. de Vries A. V., *Rec. Trav. Chim.* **77**, 441 (1958).
24. Rao, A. A., Wasan, D. T., and Manev, E. D., *Chem. Eng. Commun.* **15**, 63 (1982).
25. Angarska, J., Dimitrova, B., and Chakarova, S., to be published.
26. Dushkin, C., Tachev, K., and Angarska, J., submitted.
27. Attard, P., Mitchell, D. J., and Ninham, B. W., *J. Chem. Phys.* **89**, 4358 (1988).
28. Kralchevsky, P. A., and Paunov, V. N., *Colloids Surf.* **64**, 245 (1992).
29. Paunov, V. N., Dimova, R. I., Kralchevsky, P. A., Broze, G., and Mehreteab, A., *J. Colloid Interface Sci.* **182**, 239 (1996).
30. Israelashvili, J. N., and Wennerström, H., *J. Phys. Chem.* **96**, 520 (1992).